Development 135, 1355-1364 (2008) doi:10.1242/dev.015982

# Dual function of Src in the maintenance of adherens junctions during tracheal epithelial morphogenesis

**Masayo Shindo[1,2], Housei Wada[1], Masako Kaido[1], Minoru Tateno[1], Toshiro Aigaki,[3] Leo Tsuda[1,*] and Shigeo Hayashi[1,2,4,†]**

The downregulation of E-cadherin by Src promotes epithelial to mesenchymal transition and tumorigenesis. However, a simple loss of cell adhesion is not sufficient to explain the diverse developmental roles of Src and metastatic behavior of viral Src-transformed cells. Here, we studied the functions of endogenous and activated forms of *Drosophila* Src in the context of tracheal epithelial development, during which extensive remodeling of adherens junctions takes place. We show that Src42A is selectively activated in the adherens junctions of epithelia undergoing morphogenesis. Src42A and Src64B are required for tracheal development and to increase the rate of adherens junction turnover. The activation of Src42A caused opposing effects: it reduced the E-cadherin protein level but stimulated transcription of the E-cadherin gene through the activation of Armadillo and TCF. This TCF-dependent pathway was essential for the maintenance of E-cadherin expression and for tissue integrity under conditions of high Src activity. Our data suggest that the two opposing outcomes of Src activation on E-cadherin facilitate the efficient exchange of adherens junctions, demonstrating the key role of Src in the maintenance of epithelial integrity.

**KEY WORDS: Src, E-cadherin, Armadillo, *Drosophila*, Trachea, Cancer**

## INTRODUCTION

The concerted dissociation and re-establishment of cell-cell adhesion in epithelial cells is essential for morphogenesis, but studies of the cellular bases of those processes have begun only recently (Bertet et al., 2004; Ribeiro et al., 2004; Zallen and Wieschaus, 2004). The cell adhesion molecule E-cadherin is concentrated at the adherens junctions (AJs) and plays a key organizing role in epithelial morphogenesis (Takeichi, 1991) through its interaction with β-catenin and α-catenin, which forms a dynamically regulated molecular link between cadherins and the actin cytoskeleton (Drees et al., 2005; Yamada et al., 2005). In addition, β-catenin transduces Wnt/Wg signaling (Peifer et al., 1991) by entering the nucleus and stimulating transcription through an association with TCF (Molenaar et al., 1996). Whether cell junctions act as an alternate trigger for signaling through Armadillo (Arm) is not understood.

Members of the Src family of non-receptor protein tyrosine kinases (SFK) represent good candidates for regulators of AJ function (Thomas and Brugge, 1997). The activation of Src in cultured epithelial cells downregulates E-cadherin and causes cell dissociation (Behrens et al., 1993), and is implicated in the promotion of the epithelial-mesenchymal transition (EMT) (Boyer et al., 1997). By contrast, a recent study suggests that Src might also act positively on cell adhesion (McLachlan et al., 2007). Src elicits effects on a number of signaling pathways and multiple mammalian SFKs have overlapping functions, making genetic analyses via gene disruption difficult (Thomas and Brugge, 1997). Thus, functional studies of mammalian SFKs in the context of epithelial morphogenesis have progressed slowly.

Here, we used the *Drosophila* tracheal system to study the role of Src in epithelial morphogenesis. This respiratory system is formed by a series of dynamic remodeling steps of the tubular ectodermal epithelia (Samakovlis et al., 1996) to form a complex three-dimensional tubular network that infiltrates the entire body cavity of the larva. All of these processes occur in the absence of cell division and proceed seamlessly without the loss of epithelial integrity because of efficient cell rearrangement and the remodeling of cell junctions. Tracheal cell adhesion is defective in E-cadherin mutants (Tanaka-Matakatsu et al., 1996; Uemura et al., 1996), and the inhibition of E-cadherin turnover via elevated Rac GTPase activity causes disintegration of the tracheal epithelium (Chihara et al., 2003), suggesting that E-cadherin is a key modulator of cell adhesion in the trachea.

This prompted us to study how *Drosophila* homologs of Src (Simon et al., 1985; Takahashi et al., 2005) might regulate adherens junction turnover. We provide evidence that Src42A is preferentially activated in the AJs of epithelia undergoing morphogenesis. Src42A activation influences E-cadherin in two distinct, and disparate, ways, in that it antagonizes E-cadherin-mediated cell adhesion while simultaneously stimulating the transcription of E-cadherin. These two opposing outcomes are accompanied by an increased mobilization of AJs. We propose that the activation of Src42A in AJs promotes adherens junction turnover, thereby promoting cell rearrangement in rapidly remodeling epithelial tissues.

## MATERIALS AND METHODS

### Gene search screening

We used Gene Search (GS), based on the Gal4-UAS system (Sakata et al., 2004; Toba et al., 1999), to screen for gene activities causing EMT-like transformation in tracheal cells. In an initial screen, 5858 independent insertion lines of $UAS_G$-containing GS elements were crossed with an eye-specific *GMR-Gal4* driver to select lines causing dominant phenotypes in the eye. Next, 380 lines having the rough eye phenotype were crossed to a

[1]Riken Center for Developmental Biology, 2-2-3 Minatojima-minamimachi, Chuo-ku Kobe 650-0047, Japan. [2]National Institute of Genetics and the Graduate School for Advanced Studies, 1111 Yata, Mishima, Shizuoka-ken 411-8540, Japan. [3]Department of Biology, Tokyo Metropolitan University, Minami-Ohsawa 1-1, Hachioji, Tokyo 192-0397, Japan. [4]Department of Life Science, Kobe University Graduate School of Sciences and Technology, Kobe 657-8501, Japan.

*Present address: Department of Mechanism of Aging, National Institute for Longevity Sciences, Obu, Aichi 474-8522, Japan
†Author for correspondence (e-mail: shayashi@cdb.riken.jp)

**Accepted 24 January 2008**

strain carrying the trachea-specific *btl-Gal4* driver and the *UAS-GFP-moesin* marker. An additional 142 lines lacking the rough eye phenotype were also tested. GS11022 (*Src42A*) and GS9618 (*Src64B*) were analyzed for further study.

### Fly stocks and genetics

We used strong loss-of-function alleles of Src genes: $Src42A^{26\text{-}1}$ (Takahashi et al., 2005), $Src42A^{myri}$ (Tateno et al., 2000) and $Src64B^{P1}$ (Dodson et al., 1998). The following strains were used in this study: *trachealess* enhancer trap line *1-eve-1* (Perrimon et al., 1991), *UAS-wg* (Lawrence et al., 1995), $UAS\text{-}arm^{S10}$ (Pai et al., 1997), *UAS-TCFΔN* (van de Wetering et al., 1997), *UAS-E-cadherin-GFP* (Oda and Tsukita, 1999b), *UAS-Dα-catenin-GFP* (Oda and Tsukita, 1999a), *shg-lacZ* (Uemura et al., 1996), *UAS-GFP-moesin* (Chihara et al., 2003), *UAS-* $Src42A^{YF}$ (Tateno et al., 2000), *UAS-Src42A-RNAi* (NIG Stock Center) and *btl-Gal4* (Shiga et al., 1996). $Src42A^{DN}$ was constructed by introducing the K295M mutation at the catalytic center of the kinase domain and was cloned into the pUAST vector (Brand and Perrimon, 1993).

### Immunostaining and imaging

The following primary antibodies were used: rat anti-Esg (Fuse et al., 1994); mouse anti-tracheal luminal antigen 2A12, mouse anti-Armadillo N27A1 and mouse anti-septin 4C9H4 (Developmental Studies Hybridoma Bank); rabbit anti-β-galactosidase (Cappel); mouse anti-GFP B-2 and rabbit anti-GFP (MBL); rabbit anti-Src PY418 (Biosource International); rat anti-E-cadherin (DCAD2) (Oda et al., 1994) and rabbit anti-Src42A (Takahashi et al., 2005). Chicken anti-Src42A antibody was raised against the full-length GST-Src42A protein. For cell surface staining, S2 cells transfected with an E-cadherin-GFP expression vector, with or without Src42A vectors, were fixed with ice-cold 4% paraformaldehyde in PBS for 10 minutes. After blocking with 1% BSA in PBS, the cells were incubated with DCAD2 antibody in PBS. After washing, the cells were permeabilized by 0.1% Triton X-100 in BSA+PBS, and processed with the standard procedure to detect GFP and DCAD2. Immunostaining was detected with secondary antibodies labeled with Alexa 488 (Molecular Probes), Cy3 or Cy5 (Amersham Biosciences). Stained specimens were mounted in Vectorshield (with DAPI, Vector Laboratories) and imaged using confocal microscopes (Olympus FV500 and Olympus FV1000) with a water immersion objective [60×, numerical aperture (NA) 1.2]. Time-lapse images were obtained using a confocal microscopes equipped with a motorized stage (Olympus FV1000) and an oil immersion objective (60×, NA 1.42). Typically 20-25 1-μm optical sections were taken every 180 seconds for up to 6 hours at 25°C and projected images were converted to QuickTime movies as previously described (Kato et al., 2004). FRAP experiment was performed on the dorsal branch (DB) of stage 12 embryos (*btl>Dα-catenin-GFP* and *btl>E-cadherin-GFP*) using a confocal microscope equipped with two scanners (Olympus FV1000). GFP signal in a part of the AJ was photo bleached by 405-nm diode laser irradiation and images were taken by continuous recording (256×192 pixel, 3 *z*-stacks/frame/2.6 seconds). Image stacks were processed by iSEMS software (Wada et al., 2007) in order to computationally compensate for the vigorous movement of tracheal cells during recording. A fluorescence recovery curve was drawn according to Rabut and Ellenberg (Rabut and Ellenberg, 2005). The statistical significance of the difference between $t_{1/2}$ and $M_f$ values of control and experimental data was evaluated by Student's *t*-test (two-sided). Six control, 5 $Src42A^{myri}$, 11 $Src42A^{myri}$; $Src64^{P1}$, 10 $Src42A^{RNAi}$ and 10 $Src42A^{ACT}$ *btl>Dα-catenin-GFP* embryos were used.

### Cell culture, western blotting and immunoprecipitation

For transient transfections of S2 cells, $10^6$ cells were cultured in 35-mm culture dishes for 24 hours and then transfected with pUAST-based expression vectors and the actin 5C-Gal4 driver (generous gift of Dr Yash Hiromi, National Institute of Genetics, Mishima, Shizuoka-ken, Japan) using Effectene (Qiagen). $Src42A^{ACT}$ has a Y511F mutation, and a fly strain carrying its UAS construct (Tateno et al., 2000) was used for tracheal experiments. Two days after transfection, cells were lysed in 150 μl lysis buffer [1.0% (w/v) NP40, 0.5% deoxycholate, 150 mM NaCl, 50 mM Tris-HCl, pH 8.0] containing protease inhibitor cocktail (Complete Mini, Roche). Cell lysates were cleared by centrifugation at 20,000 ***g*** for 10 minutes, and the supernatants immunoprecipitated for 12 hours with anti-GFP beads (MBL) or anti-Arm bound to 10 μl of protein G Sepharose 4B beads at 4°C, and then subjected to SDS-PAGE and western blotting. For some western blotting experiments, *UAS-lacZ* was included as an internal control for transfection efficiency; this confirmed that the change in E-cadherin level upon elevation or reduction of Src42A activity was robust (data not shown). Surface biotinylation was performed with Sulfo-NHS-Biotin (Pierce), as described by the manufacturer.

### mRNA quantification

Poly A+ mRNA, isolated from 30 embryos using an mRNA purification kit (Amersham Biosciences), was reverse transcribed with SuperScript II (Invitrogen) reverse transcriptase using oligo-dT as a primer. mRNA was quantified using a Prism 7000 Sequence Detection System (ABI) with SYBR Green PCR Master mix (ABI). Data obtained from duplicate mRNA preparations were standardized using *rac1* mRNA as an internal control.

## RESULTS

### Src42A is activated in epithelia undergoing morphogenesis

Two *Drosophila* Src homologs, *Src42A* and *Src64B*, were identified from a gain-of-function screen for genes that alter epithelial morphology in the trachea (see Materials and methods). To monitor Src activity in *Drosophila* tissues, we used antibodies directed to the phosphotyrosine residue of Src that is essential for its activation (Y400 of Src42A, hereafter called pSrc; Fig. 1A) (Kmiecik and Shalloway, 1987; Piwnica-Worms et al., 1987). pSrc was detected preferentially in AJs of epithelial tissues (Fig. 1B-D), whereas the anti-Src42A antibody detected signals outlining many types of cells (Fig. 1D) (Takahashi et al., 2005). Both of these signals were greatly reduced in the deletion mutant $Src42A^{26\text{-}1}$ (Fig. 1E), and the low-level signal detected in this mutant may reflect maternal Src42A. Overexpression of *Src42A* in the trachea greatly increased the pSrc signal and caused a loss of epithelial integrity (Fig. 1F). Overexpression of Src64B caused a similar tracheal defect but did not significantly affect pSrc staining (Fig. 1G), most likely because the amino acid sequence in the vicinity of the Src64B autophosphorylation site (Y416) differs from that of Src42A. We conclude that the observed pSrc staining mainly represents the activation of Src42A in AJs, although a minor contribution by other proteins cannot be ruled out.

During tracheal development, pSrc expression became elevated in invaginating tracheal primordia (Fig. 1B) and its expression continued in tracheal branches undergoing cell rearrangement (Fig. 1D). pSrc staining was highly enriched in epithelial tissues undergoing various morphogenetic processes, including in the segmental furrow (Fig. 1D, arrowhead), the hindgut, the posterior spiracle and the salivary gland (data not shown). The parasegmental groove is the first morphological sign of segmentation and is formed by a transient inward shift of the apical cell surface and nucleus (Fig. 1H). pSrc was enriched in this groove (Fig. 1H) but was subsequently reduced when the groove reverted to a flat epithelia (data not shown). These observations demonstrated that Src activity is dynamically upregulated in the AJs of tissues undergoing morphogenesis.

### Src is required for tracheal cell morphogenesis

To investigate the role of Src epithelial morphogenesis, we assessed loss-of-function phenotypes of Src in the embryonic tracheal system (Fig. 2; see also Movies 1-4 in the supplementary material). Extensive cell rearrangement is involved in partitioning the proper number of cells to each of the primary branches, and later in converting multicellular tubules into unicellular ones, as revealed by single lines of the AJ marker α-catenin-GFP (Fig. 2A) (Ribeiro et

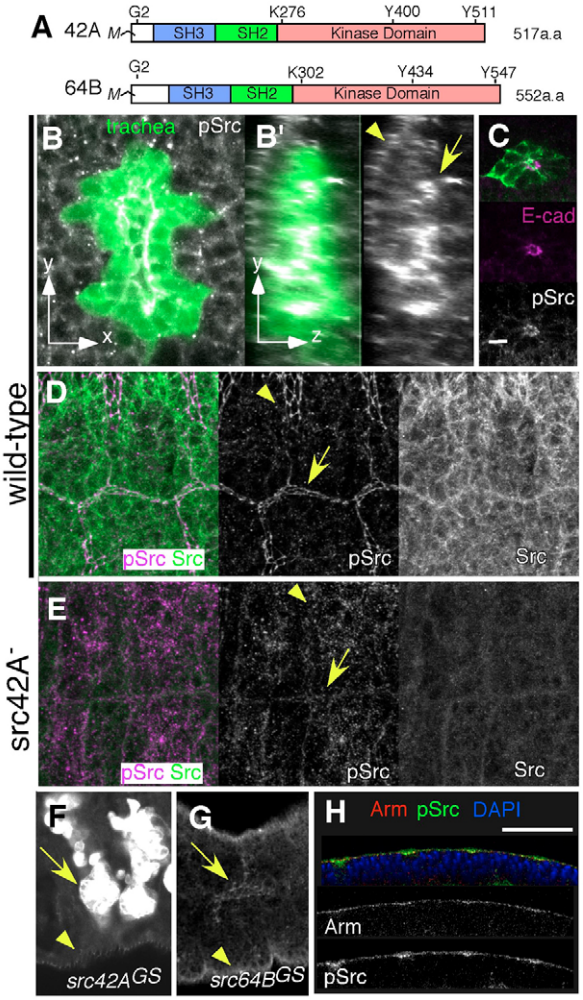


**Fig. 1. Expression of phosphorylated Src42A (pSrc) in the adherens junctions of epithelial tissues.** (**A**) Schematic diagrams of Src42A and Src64B. Three functional domains (SH3, SH2 and the kinase domain), the myristoylation (M) site at glycine 2 (G2), the catalytic lysine in the kinase domain, and the sites of activating (Y400/434) and inhibitory (Y511/547) tyrosine phosphorylation are indicated. (**B-D**) Staining pattern of anti-phospho Src (pSrc) antibody during tracheal development. (B) Embryos were stained for pSrc (gray scale), and tracheal cells were labeled green with *trh-lacZ*. pSrc was localized to the apical cell-cell junction of the ectoderm and in invaginating tracheal primordia in stage 11. (B′) *y-z* section shows that tracheal cells (arrow) express a higher level of pSrc than ectoderm (arrowhead). (C) pSrc and E-cadherin are co-localized in the AJs of stage 11 tracheal primordia (*btl>gfp-moe*, green). (D) Src expression in a control ($Src42A^{26\text{-}1}$/+) embryo at stage 14, showing broad cell membrane staining by anti-Src42A antibody and highly restricted AJ staining by anti-pSrc (arrow indicates trachea; arrowhead, epidermis). (**E**) Both signals were greatly reduced in $Src42A^{26\text{-}1}$ mutant embryos. (**F**) Src42A overexpression in the trachea (*btl>*$Src42A^{GS}$) greatly increased the pSrc signal (arrow). (**G**) Src64B overexpression in the trachea (*btl>* $Src64B^{GS}$) did not increase the pSrc signal. (**H**) Src activation in the parasegmental furrow. Optical section of the embryonic ectoderm at stage 9 labeled with pSrc (green) and Arm (magenta). Nuclei were visualized by DAPI (blue). Grayscale images of the two channels are shown below. Scale bars: in C, 10 μm for B,C; in H, 100 μm.

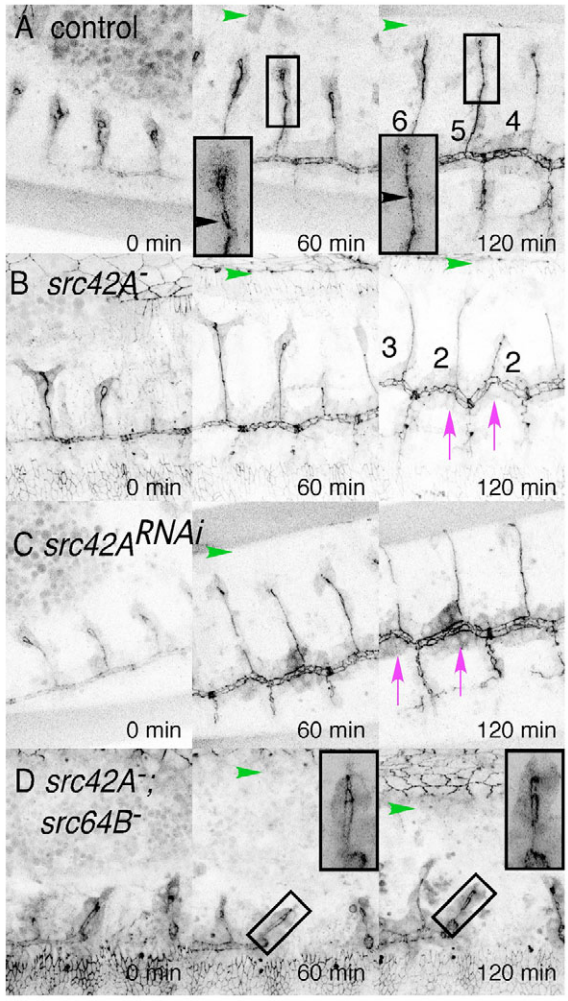


**Fig. 2. Requirement for Src functions in tracheal morphogenesis.** (**A-D**) Snap-shot images from a time-lapse series of tracheae labeled with α-catenin-GFP (see also Movies 1-4 in the supplementary material). Genotypes are: control (A), $Src42A^{myri}$ (B), *btl>*$Src42A^{RNAi}$; $Src42A^{26\text{-}1}$/+ (C) and $Src42A^{myri}$; $Src64B^{P1}$ (D). Arrows in magenta indicate the position of a dorsal trunk 'bend', which is likely to be due to an excessive pulling force applied by the shortened dorsal branch. Green arrowheads indicate the position of the leading edge of dorsal epidermis. Inset shows an enlarged view of AJs in the dorsal branch. The images represent more than three independent embryos of each genotype.

al., 2004). The dorsal branch (DB) 1 to 9 consists of a pair of cells at the tip (fusion cell and terminal cell) and 2 to 7 stalk cells (4.3±0.03, $n$=44), and is extended in concert with dorsal closure (DC) of the epidermis (Fig. 2A) (Kato et al., 2004). In $Src42A^{myri}$ mutant embryos, the DB lagged behind DC and contained fewer stalk cells (2.6±0.02, $n$=46, $P<3\times10^{-10}$; two-sided Student's $t$-test; Fig. 2B). The dorsal trunk (DT) became a zigzag shape, indicating that increased pulling forces applied by the shortened DBs deformed the DT. To test whether the phenotype of $Src42A^{myri}$ reflects a trachea-autonomous function of Src42A, we reduced *Src42A* expression by expressing a hairpin RNA construct of *Src42A* (see Fig. S1 in the supplementary material for its effect in the wing disc) and removing one zygotic copy of *Src42A*. The mutants reproduced the *Src42A* loss-of-function phenotype in the trachea. The number of stalk cells was reduced (3.6±0.1, $n$=9, $P$<0.05) and the phenotypes of delayed DB extension and zigzagged DT were observed (Fig. 2C). Further reduction of Src function by the $Src42A^{myri}$; $Src64B^{P1}$ double mutation exacerbated the phenotype.

Many DBs were arrested in a multicellular state despite the progression of DC (Fig. 2D). The phenotype in the trachea was much more severe than the relatively minor defects observed in dorsal closure (Takahashi et al., 2005). Perhaps the prolific rearrangement of cells in the trachea makes this tissue highly sensitive to changes in Src activity. The expression of Spalt, which inhibits cell rearrangement (Ribeiro et al., 2004), remained limited to the DT (see Fig. S2 in the supplementary material), suggesting that the transformation of branch-specific cell fate is unlikely to account for the phenotype. In summary, the reduction of Src activity caused a variety of phenotypes in the DBs, including the reduction of cell number, delayed branch extension and delayed cell intercalation.

## Antagonistic interaction of Src and E-cadherin in tracheal branch migration

To investigate whether the observed phenotypes of Src mutants involve E-cadherin, we altered the activities of E-cadherin and Src42A in the trachea and examined their effect on cell rearrangement and adhesion. We first revisited the tracheal phenotypes of mutants of the E-cadherin gene *shotgun* (*shg*), using live imaging of α-catenin-GFP, which has been used as a marker for AJs (Oda and Tsukita, 1999a; Ribeiro et al., 2004). Although E-cadherin is a core component of AJs, whether its production is rate limiting in junctional remodeling in embryos has not been well clarified because zygotic *shg* mutants undergo a substantial degree of epithelial morphogenesis, including the formation of apparent unicellular branches (Tepass et al., 1996; Uemura et al., 1996). However, in time-lapse images of *shg* mutants, we noted that AJ signals became increasingly faint and discontinuous, and that cell attachment in the tracheal branches was loosened and broken at several places (Fig. 3C, compare with Fig. 3B; see also Movie 5 in the supplementary material). These phenotypes were more severe in the unicellular DB than in the multicellular DT (Fig. 3C). We next increased the dosage of E-cadherin several fold by expressing the E-cadherin-GFP fusion protein in tracheal cells, and then compared its effect on DB elongation with that of control GFP-moesin-expressing embryos (Fig. 3A,D; see also Movies 6, 7 in the supplementary material). E-cadherin-GFP delayed elongation of the DBs (Fig. 3I) and cell rearrangement, as evidenced by the fact that a multicellular tubule still remained after 3 hours of recording (Fig. 3D, inset, arrowhead marking dual lines of the AJ; compare with Fig. 3A), suggesting that excess E-cadherin is inhibitory to the morphogenesis of DBs. Despite the delay, tracheal development was eventually completed (Oda and Tsukita, 1999b). These results suggest that the expression of E-cadherin must be maintained at a proper level to allow the smooth morphogenesis of unicellular DB.

We next studied the role of activated Src in E-cadherin-dependent cell adhesion. Src42A$^{ACT}$ caused disintegration of the tracheal epithelium in a manner similar to that of Src42A or Src64B overexpression (Fig. 3E; see also Movie 6 in the supplementary material). Src42A$^{ACT}$-expressing trachea marked with AJ markers (GFP-moesin, α-catenin-GFP, E-cadherin-GFP; Fig. 3E,F,H) had rounded cells and discontinuous luminal cavities with deteriorating apicobasal polarity, and an occasional detachment of the tip cells of the DBs (Fig. 3F). Time-lapse recordings demonstrated that tracheal cells expressing Src42A$^{ACT}$ failed to stabilize cell junctions and to extend branches, although they retained filopodia activity (see

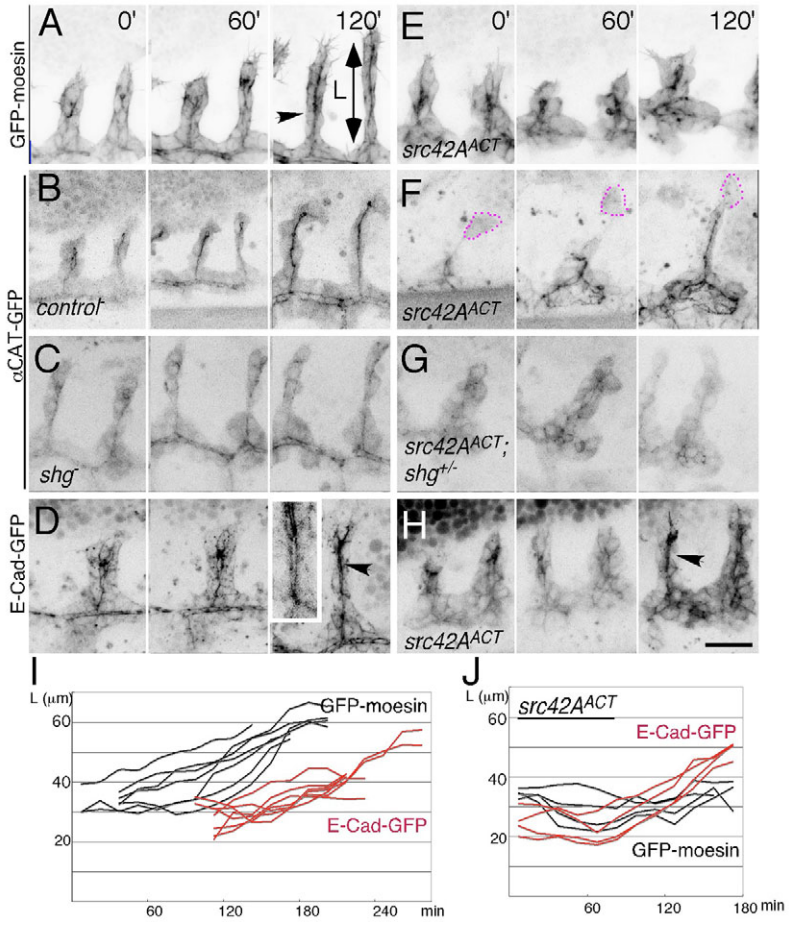


**Fig. 3. Src antagonizes E-cadherin during tracheal branching.** (**A-D**) Dorsal branch morphologies in embryos with various levels of E-cadherin. Markers and genotypes are indicated on the left. (A) Control embryos carrying *btl>GFP-moesin*. Arrowhead indicates the lumen. L, length of dorsal branch (DB) measured and plotted in I and H. (B) Control embryos carrying *btl>α-catenin-GFP* that labels the AJ as a black line in each dorsal branch. (C) In *shg$^{IH}$/shg$^{E17B}$* mutants, AJs became diffuse and discontinuous. (D) E-cadherin-GFP-expressing tracheae undergo slightly delayed, but morphologically normal, branching. Inset shows double lines of AJs remaining in the late stage of DB elongation. (**E-H**) Effect of activated Src42A on dorsal branch morphology and AJs. (E) In embryos expressing activated Src42A, tracheal cell contact persisted but became loose, and the lumen became discontinuous. (F) *Src42A$^{ACT}$* loosened AJs. Dotted circles indicate transiently detached cells at the tip of the DB. (G) This phenotype was further enhanced in the *shg$^{IH}$*/+ background. Most cells have now rounded up and lost accumulation of *α-catenin-GFP*. (H) E-cadherin-GFP partially restored the extent of elongation of the DB and its lumen (compare with E). (**I**) Plot of the length of DBs (L, see A). The onset of DT fusion was set as time 0 for each measurement. When compared with DBs labeled with GFP-moesin, E-cadherin-GFP delayed DB elongation in an otherwise wild-type background. (**J**) E-cadherin-GFP partially restores elongation of DBs expressing Src42A$^{ACT}$. Original movies for A, C, D, E and H are presented as Movies 5-7 in the supplementary material. Scale bar in H: 25 μm.

Movies 6, 7 in the supplementary material). The reduction of one of the zygotic copies of *shg* enhanced the phenotype of Src42A$^{ACT}$: DTs were broken at many places, AJ accumulation of α-catenin-GFP was much reduced and cells were more rounded (compare Fig. 3G with 3F). Furthermore, co-expression of E-cadherin-GFP significantly restored the branch elongation defects that were due to Src42A$^{ACT}$ (see Fig. 3E,H,J). The tracheal cells maintained apicobasal polarity for at least 2 hours longer and dorsal branches were extended (Fig. 3H), indicating that a high level of E-cadherin partially suppresses the effect of Src42A$^{ACT}$. The results suggest that E-cadherin is a rate-limiting component of Src42A-mediated cell junctional destabilization.

## The turnover of AJs depends on Src

To study the effects of Src on the dynamics of AJs, we performed a FRAP (fluorescence recovery after photobleaching) analysis of AJs (Fig. 4A-C). In control embryos, fluorescence of α-catenin-GFP recovered to 30.6% (±2.2, $n$=6) of the original level, with the half time of recovery ($t_{1/2}$) being 16.7±1.6 seconds (Fig. 4D). These values were in the same order as those obtained for E-cadherin-GFP [mobile fraction ($M_f$)=34.7±9.5 %, $t_{1/2}$=23.7±6.8 seconds] and in good agreement with the values obtained from mammalian tissue culture cells (Yamada et al., 2005). Because a change of E-cadherin level altered tracheal branch migration (Fig. 3), we chose α-catenin-GFP as a neutral marker of AJs for subsequent FRAP analyses.

As shown in Fig. 4D, the mild reduction of Src activity in the *Src42A$^{miri}$* mutant did not significantly alter $t_{1/2}$ and $M_f$. However, upon strong reduction of Src activity by a *Src42A; Src64B* double mutation, $t_{1/2}$ was increased to 28.1 seconds ($P$>0.05), while $M_f$ was not significantly altered. Furthermore, tracheal-specific RNAi knockdown of *Src42A* (*btl>Src42A$^{RNAi}$*) increased $t_{1/2}$ (22.0 seconds, $P$<0.05), suggesting that cell-autonomous activity of Src42A contributes to the fast turnover of AJs. By contrast, Src42A$^{ACT}$ increased $M_f$ to 56.2% ($P$>0.005). Src42A$^{ACT}$ also increased $t_{1/2}$, probably to due to the increased $M_f$. Unlike Src double mutants, *btl>Src42A$^{RNAi}$* slightly increased $M_f$. The difference between the two Src loss-of-function conditions might be due to the persistent presence of tension applied by wild-type tissues in *btl>Src42A$^{RNAi}$*. Taken together, the results demonstrate that Src is required for mobilization of the AJs.

## Src downregulates E-cadherin and Armadillo

To study the regulation of E-cadherin and Arm by Src in a defined system, we used *Drosophila* S2 cells. Expressed E-cadherin-GFP stabilized endogenous Arm (Fig. 5A. The amounts of both E-cadherin and Arm were reduced by Src42A$^{ACT}$, and were elevated by a dominant-negative form of Src, Src42A$^{DN}$ (Fig. 5A,B). Src42A$^{ACT}$ specifically reduced the amount of the slower mobility form of Arm that was known to be hyperphosphorylated (Fig. 5A, band labeled H). As revealed by cell surface antibody staining and cell surface biotinylation (Fig. 5B,C; see also Materials and methods), Src42A$^{ACT}$ was found to deplete E-cadherin from the cell surface, and, consequently, resulted in a loss of cell adhesion (Fig. 5B, data not shown). It was previously shown that the E-cadherin/Arm complex includes Src42A (Takahashi et al., 2005). We now found that immunoprecipitated Arm includes Src42A (Fig. 5A). Src42A$^{DN}$ in whole-cell extract reacted with pSrc, possibly as a result of transphosphorylation by endogenous Src proteins. However, Y400 of Src42A, which associates with Arm, was under phosphorylated in Src42A$^{DN}$ cells and hyperphosphorylated in Src42A$^{ACT}$ cells (Fig. 5A), suggesting that the Y400 phosphorylation status of Src42A bound to Arm inversely correlates with cell adhesion activity. In embryos lacking most of the zygotic Src activities (*Src42A$^{myri}$, Src64B$^{P1}$* double-mutants), we observed an ~70% increase of E-cadherin protein (Fig. 5D). These observations suggest that Src proteins normally downregulate E-cadherin.

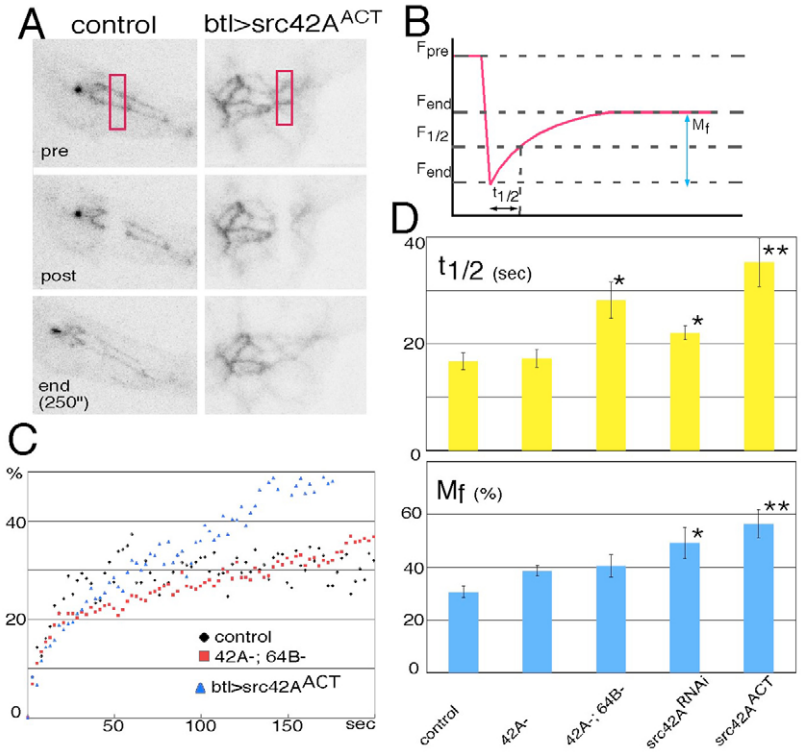


**Fig. 4. FRAP analyses of α-catenin-GFP.** (**A**) Dorsal branch of *btl>α-catenin-GFP* embryos with or without Src42A$^{ACT}$ were photo bleached at the bracketed regions and fluorescence recovery was recorded. (**B**) Schematic plot of FRAP analysis. Photo bleaching reduces the fluorescence level from pre bleach ($F_{pre}$) to post bleach ($F_{post}$). Fast recovery of fluorescence reaches an approximate plateau level ($F_{end}$) that is usually lower than $F_{pre}$. Recovery to $F_{pre}$ required a longer time and was not analyzed. Mobile fraction [$M_f$=100×($F_{end}$–$F_{post}$)/($F_{pre}$–$F_{post}$)] and half-time of recovery ($t_{1/2}$) were estimated from the plots. (**C**) Representative plots of fluorescence recovery in dorsal branches of control (black), *Src42A; Src64B* double mutant (red) and Src42A$^{ACT}$-expressing (blue) embryos. (**D**) $t_{1/2}$ and $M_f$ values under various conditions of Src activities. Error bar indicates standard error. Values that deviate from controls are indicated (*$P$<0.05, **$P$<0.005).

## Src upregulates E-cadherin transcription

The results so far demonstrated that Src is a negative regulator of E-cadherin and AJs. However, the effect Src on the level of E-cadherin protein was modest: by antibody staining only a small change in the level of E-cadherin protein in tracheal cells was observed in Src mutants (data not shown). To explore the additional control of E-cadherin by Src, we studied Arm. In wild-type embryos, Arm is localized at apical cell-cell adhesion sites in a pattern similar to that of E-cadherin (Fig. 6A). In contrast to the observation in S2 cells (Fig. 5A), Src42A$^{ACT}$ increased the Arm signal in tracheal cell cytoplasm (Fig. 6D). Furthermore, Src42A$^{ACT}$ greatly increased the expression of Escargot (Esg), a known target of Wg/Arm signaling in the trachea (Chihara and Hayashi, 2000; Llimargas, 2000) (Fig. 6B,E,L), whereas *Src42A$^{myri}$* mutants reduced expression (Fig. 6H). Thus, Src42A stimulates Esg expression in the trachea. The transcription factor TCF acts downstream of Arm (van de Wetering et al., 1997). Its dominant-negative form, TCFΔN, suppressed the increase in the number of Esg-expressing cells caused by Src42A hyperactivation (Fig. 6J), suggesting that Src activates Esg through the Arm-TCF pathway.

In our search for additional Src42A targets in the trachea, we identified E-cadherin. The transcriptional reporter gene *shg-lacZ* was detected in all tracheal cells, and its expression was elevated in fusion cells, where E-cadherin is upregulated (Fig. 6C) (Tanaka-Matakatsu et al., 1996). *shg-lacZ* expression was greatly stimulated by the hyperactivation of Wg signaling (Fig. 6M), and was reduced by TCFΔN (Fig. 6I), further suggesting that *shg* is regulated by the canonical Wg pathway. *shg-lacZ* was also stimulated by Src42A$^{ACT}$ in a TCF-dependent manner (Fig. 6F,K). The positive effect of Src42A on E-cadherin transcription was confirmed by the direct measurement of E-cadherin mRNA in embryos ubiquitously expressing Src42A$^{ACT}$ or wild-type Src42A (Src42A$^{GS}$, Fig. 6N). Src42A$^{ACT}$ and Src42A$^{GS}$ increased E-cadherin mRNA by about threefold, comparable to induction by Wg, whereas the level of control mRNA (*rac1*) did not change significantly (Fig. 6N). Additionally, Src42A increased *arm* mRNA in these embryos (Fig. 6N). These results suggest that Src42A upregulates E-cadherin and Esg transcription via the transcriptional activation and stabilization of Arm.

## Antagonistic activities of the Src42A and Wnt pathway on tracheal cell adhesion

Our analyses identified two opposing effects of Src on AJs: the inhibition of cell adhesion and the upregulation of E-cadherin by stimulating its transcription by activating Arm and TCF. Although Src42A$^{ACT}$ strongly destabilized cell adhesion, it did not cause complete cell dissociation (Fig. 3E,F,H). In some cases, we observed Src42A$^{ACT}$-expressing tracheal cells that were detached from one branch and re-attached to the neighboring branch, suggesting that Src42A$^{ACT}$-expressing tracheal cells retain a significant level of homophilic cell adhesion (Fig. 7A; see also Movie 8 in the supplementary material). We speculated that the elevated synthesis of E-cadherin would have compensated for its inactivation upon hyperactivation of Src42A, thereby preventing the complete diminution of cell adhesion. Consistent with this idea, we found that the *shg* mutation enhanced the effect of Src42A$^{ACT}$; tracheal cells were now completely dissociated (Fig. 7E). To specifically address the significance of Src-mediated activation of Arm, we observed the phenotype of TCFΔN overexpression. TCFΔN blocked tracheal branching, but did not disrupt epithelial integrity (Fig. 7C), suggesting that the downregulation of TCF-dependent expression of E-cadherin was not rate limiting at the normal level of Src activity.

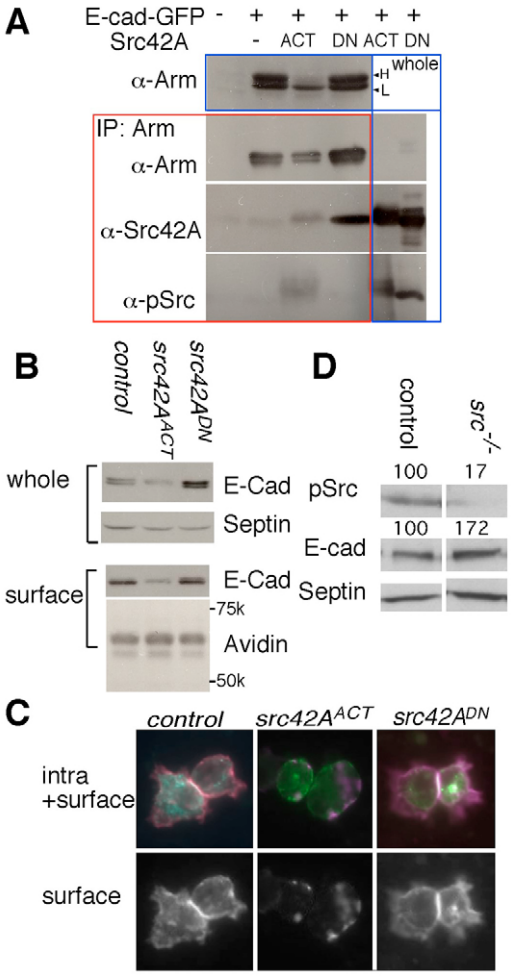


**Fig. 5. Regulation of E-cadherin-catenin complex by Src42A.** (**A**) Complex formation by E-cadherin, Arm and Src42A. Expression constructs of E-cadherin-GFP and Src42A were transfected into S2 cells and the E-cadherin-Arm complex was analyzed by immunoprecipitation. Blue and red boxes mark the lanes of whole cell extract and immunoprecipitates of anti-Arm, respectively. The expression of E-cadherin-GFP stabilized Arm in apparent high and low molecular weight forms, indicated by H and L. Although both Src42A$^{ACT}$ and Src42A$^{DN}$ in whole cell extract were phosphorylated at Y400, Src42A$^{DN}$ in complex with Arm was under phosphorylated. (**B**) Src42A downregulates the cell surface level of E-cadherin. Surface biotinylation was applied to S2 cells expressing E-cadherin-GFP and Src42A. Western blot analyses were performed on whole cell extracts (whole) and proteins were recovered by avidin beads (surface). Septin and avidin-reacting proteins were used as loading controls for each blot. The positions of marker proteins are shown in the avidin panel. (**C**) Downregulation of E-cadherin-GFP by Src42A$^{ACT}$. Transfected S2 cells were stained with a method to detect extracellular E-cadherin (surface, magenta). GFP signal in the intracellular domain (intra, green) is shown. Src42A$^{ACT}$ reduced both signals. (**D**) The amount of E-cadherin was reduced in Src mutant embryos. Control and *Src42A$^{myr}$; Src64B$^{P1}$* embryos (*src$^{-/-}$*) were collected and analyzed for E-cadherin and pSrc expression by western blotting. Protein extracts were analyzed in the same gels and blots. Relative amount is shown above each band.

Strikingly, Src42A$^{ACT}$ and TCFΔN co-expression synergistically caused tracheal cells to lose cell polarity and dissociate (Fig. 7F; Movie 9 in the supplementary material). Antibody staining of these embryos demonstrated that Src42A$^{ACT}$ mildly reduced E-cadherin.

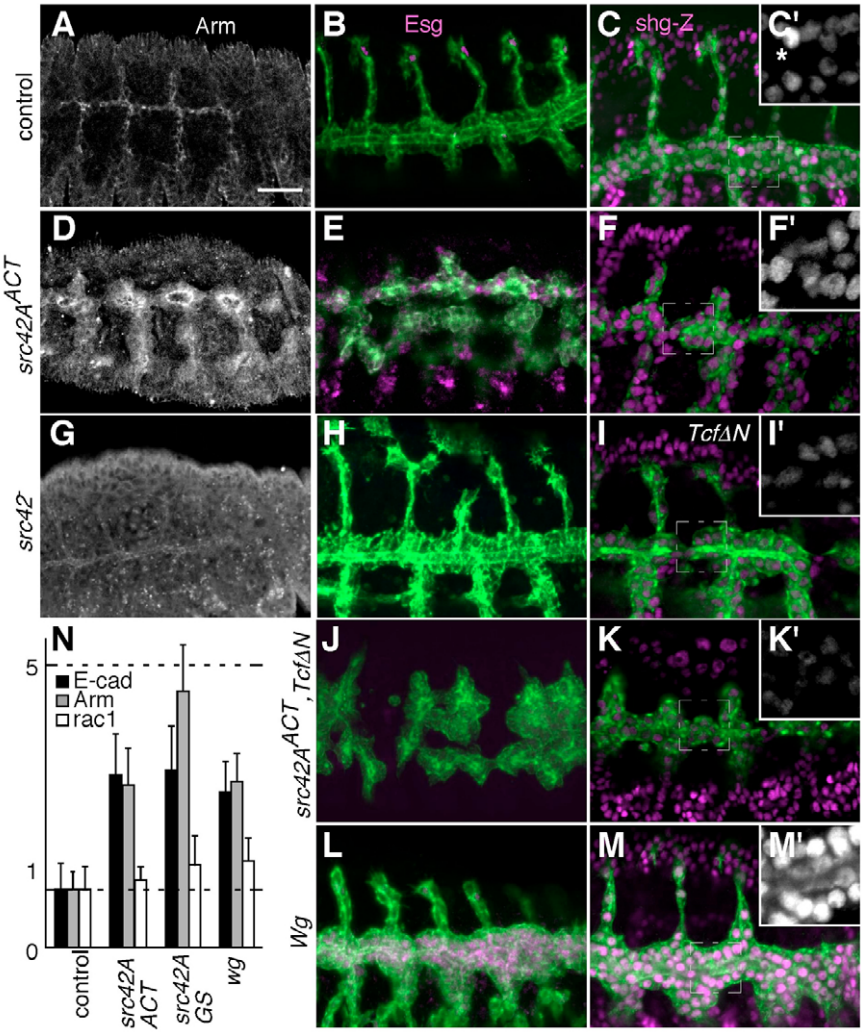


**Fig. 6. Src activates E-cadherin transcription through Arm.** (**A-C**) Control; (**D-F**) *btl>Src42A$^{ACT}$*; (**G**,**H**) *Src42A$^{myr}$*; (**I**) *btl>TCFΔN*; (**J**,**K**) *btl>TCFΔN+Src42A$^{ACT}$*; (**L**,**M**) *btl>wg*. Tracheal cells are labeled with *btl>GFP-moesin* (green). (A,D,G) Arm (grayscale) is localized to the apical cell-cell junction in control embryos (A). In *Src42A$^{ACT}$* embryos, the Arm signal increased to fill the entire tracheal cell (D). Arm staining was reduced in *Src42A* mutants (G). (B,E,H,J,L) Esg expression (magenta) was localized to fusion cells in control embryos (B), and the number of Esg-expressing cells was greatly increased in embryos overexpressing *Src42A$^{ACT}$* or *wg* (E,L). In *Src42A$^{myr}$* or *Src42A$^{ACT}$*, *TCFΔN* embryos, Esg was almost undetectable (H,J). (C,F,I,K,M) *shg-lacZ* (nuclear signal, magenta) was broadly expressed, with elevated levels in tracheal fusion cells (C, asterisk in C′). (C′-M′) Framed area in C-M enlarged and shown in grayscale. The number of strong *shg-lacZ*-expressing cells increased in embryos overexpressing *Src42A$^{ACT}$* or *wg* (F,M). In *Src42A$^{myr}$* or *Src42A$^{ACT}$*, *TCFΔN* embryos, *shg-lacZ* expression was reduced in tracheal cells (I,K; compare the levels in the trachea and ectoderm). Scale bar in A: 20 μm for A-M. (**N**) RNA quantification. *Src42A$^{ACT}$*, *Src42A$^{GS}$* or *wg* was expressed under the control of the ubiquitous *da-Gal4* driver, and the levels of E-cadherin, *arm* and *rac1* mRNAs were measured by quantitative RT-PCR. *da-Gal4* embryos were used as a control.

The additional presence of TCFΔN synergistically caused the near complete removal of E-cadherin (see Fig. S3 in the supplementary material). These results demonstrated that TCF-dependent transcription helps to maintain epithelial integrity under conditions of high Src activity.

## DISCUSSION

### Dual function Src in the turnover of AJs

The turnover of cell adhesion proteins at the AJs is a key target for regulators of tissue morphogenesis. We have shown that the dual functions of Src42A are important for coordinating the turnover of AJs during tracheal morphogenesis in *Drosophila*. The activation of Src42A promoted the downregulation of E-cadherin protein and TCF-dependent transcriptional activation of the E-cadherin gene. The dosage-sensitive interaction of Src42A$^{ACT}$ and E-cadherin suggests that E-cadherin is a rate-limiting component under the control of Src42A. The simultaneous removal and replenishment of E-cadherin at the AJs promoted by Src42A would accelerate E-cadherin turnover, as demonstrated by our FRAP analysis. The preferential association of the E-cadherin-Arm complex with an inactive form of Src42A (Fig. 5A) suggests a model in which activation of Src42A triggers inactivation of the E-cadherin-Arm complex. This idea is supported by the loss-of-function phenotypes of Src, which show defects in cell rearrangement, a reduced turnover rate of Dα-catenin-GFP, and a loss of some TCF target gene expression. We thus suggest that Src is a key coordinator of junctional remodeling in epithelia undergoing rapid cell rearrangement.

Wild-type tracheal cells undergoing rapid cell rearrangement sometimes dissociated from the tracheal system (Fig. 7B, arrowhead). Those cells stayed in the body cavity until engulfed by hemocytes. By contrast, tracheal cells expressing Src42A$^{ACT}$ and dissociated from branches acquired the ability to re-associate with other tracheal cells (Fig. 7A). The enhancement of both de-adhesion and re-adhesion by Src42A$^{ACT}$ mimics the behavior of tumor cells undergoing metastasis, suggesting that the dual function of Src42A on E-cadherin might provide a molecular clue for understanding tumor metastasis.

### The role of Src in Arm-dependent transcription

A negative role of activated Src on E-cadherin-dependent cell adhesion has been observed in cases of embryonic ectoderm undergoing dorsal closure (Takahashi et al., 2005). We noted that the cell dissociation effect of Src42A$^{ACT}$ was much stronger on tracheal epidermis than on dorsal ectoderm (S.H., unpublished). We suggest that the vigorous cell rearrangement and high level of Src42A activity in the tracheal epithelium lead to a rapid decline of E-cadherin protein, and make the de novo synthesis of E-cadherin essential, as demonstrated by the loss of AJs in *shg* mutant embryos (this study) (Tanaka-Matakatsu et al., 1996).

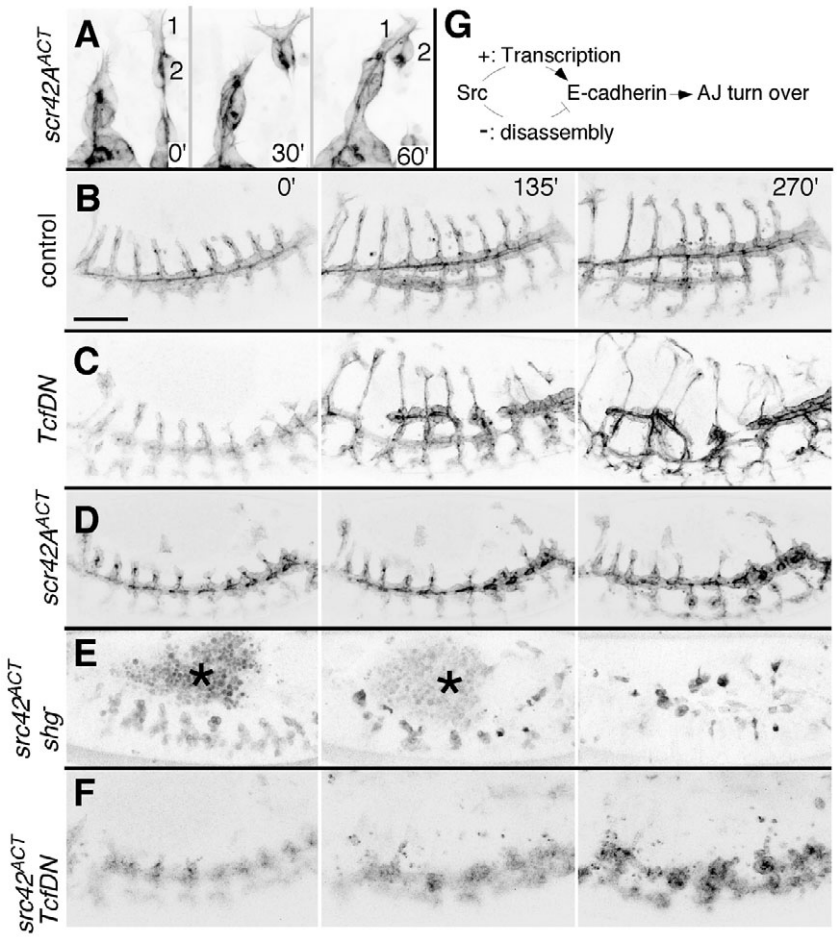


**Fig. 7. Essential role of Src-induced Arm/TCF activity in tracheal cell adhesion.** (**A-F**) Time-lapse observations of *btl>GFP-moesin* (A-D,F) or *btl>αCat-GFP* (E) in control (B), *btl>TCFΔN* (C), *btl>Src42A$^{ACT}$* (A,D), *btl>Src42A$^{ACT}$; shg$^{IH}$* (E) and *btl>Src42A$^{ACT}$*, *TCFΔN* (F) embryos. (A) Metastasis-like behavior of tracheal cells expressing Src42A$^{ACT}$. Cells numbered 1 and 2 detached from one branch and reattached to an adjacent branch. (B-E) Src42A$^{ACT}$ and TCFΔN synergistically caused a strong cell dissociation phenotype. Asterisk in E indicates the autofluorescence of yolk. Original movies for A,B,D and F are presented as Movies 8, 9 in the supplementary material. (**G**) Model of the dual function of Src42A on E-cadherin. Scale bar in B: 50 μm for B-D,F; 25 μm for E; 10 μm for A.

We have shown here that Src42A increased the accumulation of Arm and promoted the TCF-dependent stimulation of Esg and E-cadherin expression, demonstrating that Src42A plays a previously unrecognized role in stimulating the transcriptional activity of Arm. The increase of *arm* mRNA due to Src42A suggests that the activation of Arm involves a positive transcriptional feedback mechanism. Furthermore, release of Arm from the AJs, and its stabilization, may also contribute to the activation of Arm. The stimulation of E-cadherin transcription by Src42A may be a direct consequence of Arm activation, as stimulation of E-cadherin synthesis by Wg was observed in cultured *Drosophila* cells (Wodarz et al., 2006).

TCF-dependent synthesis of E-cadherin by itself was not rate limiting for tracheal cell adhesion, probably because its absence left the level of E-cadherin above the threshold to maintain cell adhesion. However, de novo synthesis of E-cadherin became essential when Src42A$^{ACT}$ accelerated the degradation of E-cadherin. The essential role of Arm-mediated transcriptional activation was most clearly illustrated by the complete cell dissociation phenotype of tracheal cells upon activation of Src42A and TCFΔN (Fig. 7). We suggest that the transcriptional stimulation of the E-cadherin gene by Arm compensates for the elevated degradation rate of E-cadherin due to Src42A$^{ACT}$.

Wg controls tracheal branching by activating Arm and the transcription of Esg (Chihara and Hayashi, 2000; Llimargas, 2000). As Esg expression also requires Src42A in the trachea, this observation suggests that the simultaneous activation of Wg and Src is required to increase the level of Arm sufficiently for the transcriptional activation of Esg. By contrast, the expression of *spalt*, another Wg target gene in the trachea, was not altered by a loss or gain of Src activity. In addition, *Src42A; Src64B* double mutant embryos did not show any segmentation defects that were characteristic of Wg class segment polarity mutations. These results suggest that the role of Src in Wg signaling is limited, perhaps because the level of Arm accumulation caused by normal levels of Src is less than the threshold of activation of most of Wg target genes.

## The regulation of Src

Although Src is known to regulate cell-matrix adhesion through the integrin pathway (Frame et al., 2002), preferential localization of pSrc in AJs indicates that AJs are the major site of Src function in *Drosophila* embryos. We have shown that pSrc is enriched in epithelia having high morphogenetic activity or undergoing sharp deformation. During tracheal development, the tip of the DB is tightly associated with the epidermis, and its elongation is coupled to dorsal closure, a unidirectional movement of the epidermis (Kato et al., 2004). This implies that branch elongation is driven at least in part by an externally applied force that generates tension in the tracheal epithelium. It was reported that the mechanical stretching of cultured cells activates Src through an interaction with actin filaments (Han et al., 2004; Wang et al., 2005). We speculate that mechanical deformation and tension applied to AJs through morphogenetic movements in tracheal development are good candidates for triggering Src activation.

## The regulation of epithelial morphogenesis by Src

Our results suggest that E-cadherin is under dual control by Src (Fig. 7G). Introducing a repressor of E-cadherin to this system would change the balance toward cell dissociation, as has been observed in Sna/Slug-induced EMT in vertebrate development (Cano et al., 2000). Thus, the effect of Src on the synthesis and degradation of E-cadherin can be modulated depending on the cellular context, and this may explain the various functions of Src in developmentally programmed EMT or in metastasis during cancer progression. We suggest that the positive and negative control of E-cadherin by Src during rapid cell rearrangements in the tracheal epithelium represent an equilibrium between epithelial and transient mesenchymal states. The widespread expression of pSrc in epithelial tissues indicates that the equilibrium state of cell adhesion is common in development, the advantage being to buffer the various mechanical stresses arising during morphogenetic movement.

We are grateful to Mayuko Nishimura and Kagayaki Kato for helping with experiments and data analyses; and to Akira Nagafuchi, Shin-ichi Nakagawa, Tetsu Otani, Tatsuhiko Noguchi and members of the Hayashi lab for discussion and comments on the manuscript. We thank Tadashi Uemura, Kaoru Saigo, Hiroki Oda, Shin-ichi Yanagawa, the Developmental Studies Hybridoma Bank, the Bloomington Stock Center and the NIG stock Center for flies, DNA and/or antibodies. This work was supported by Grant-in-Aid for Scientific Research from MEXT Japan (Systems Genomics).

### Supplementary material

Supplementary material for this article is available at
http://dev.biologists.org/cgi/content/full/135/7/1355/DC1

### References

**Behrens, J., Vakaet, L., Friis, R., Winterhager, E., Van Roy, F., Mareel, M. M. and Birchmeier, W.** (1993). Loss of epithelial differentiation and gain of invasiveness correlates with tyrosine phosphorylation of the E-cadherin/beta-catenin complex in cells transformed with a temperature-sensitive v-SRC gene. *J. Cell Biol.* **120**, 757-766.

**Bertet, C., Sulak, L. and Lecuit, T.** (2004). Myosin-dependent junction remodelling controls planar cell intercalation and axis elongation. *Nature* **429**, 667-671.

**Boyer, B., Roche, S., Denoyelle, M. and Thiery, J. P.** (1997). Src and Ras are involved in separate pathways in epithelial cell scattering. *EMBO J.* **16**, 5904-5913.

**Brand, A. H. and Perrimon, N.** (1993). Targeted gene expression as a means of altering cell fates and generating dominant phenotypes. *Development* **118**, 401-415.

**Cano, A., Perez-Moreno, M. A., Rodrigo, I., Locascio, A., Blanco, M. J., del Barrio, M. G., Portillo, F. and Nieto, M. A.** (2000). The transcription factor snail controls epithelial-mesenchymal transitions by repressing E-cadherin expression. *Nat. Cell Biol.* **2**, 76-83.

**Chihara, T. and Hayashi, S.** (2000). Control of tracheal tubulogenesis by Wingless signaling. *Development* **127**, 4433-4442.

**Chihara, T., Kato, K., Taniguchi, M., Ng, J. and Hayashi, S.** (2003). Rac promotes epithelial cell rearrangement during tracheal tubulogenesis in Drosophila. *Development* **130**, 1419-1428.

**Dodson, G. S., Guarnieri, D. J. and Simon, M. A.** (1998). Src64 is required for ovarian ring canal morphogenesis during Drosophila oogenesis. *Development* **125**, 2883-2892.

**Drees, F., Pokutta, S., Yamada, S., Nelson, W. J. and Weis, W. I.** (2005). Alpha-catenin is a molecular switch that binds E-cadherin-beta-catenin and regulates actin-filament assembly. *Cell* **123**, 903-915.

**Frame, M. C., Fincham, V. J., Carragher, N. O. and Wyke, J. A.** (2002). v-Src's hold over actin and cell adhesions. *Nat. Rev. Mol. Cell. Biol.* **3**, 233-245.

**Fuse, N., Hirose, S. and Hayashi, S.** (1994). Diploidy of Drosophila imaginal cells is maintained by a transcriptional repressor encoded by escargot. *Genes Dev.* **8**, 2270-2281.

**Han, B., Bai, X. H., Lodyga, M., Xu, J., Yang, B. B., Keshavjee, S., Post, M. and Liu, M.** (2004). Conversion of mechanical force into biochemical signaling. *J. Biol. Chem.* **279**, 54793-54801.

**Kato, K., Chihara, T. and Hayashi, S.** (2004). Hedgehog and Decapentaplegic instruct polarized growth of cell extensions in the Drosophila trachea. *Development* **131**, 5253-5261.

**Kmiecik, T. E. and Shalloway, D.** (1987). Activation and suppression of pp60c-src transforming ability by mutation of its primary sites of tyrosine phosphorylation. *Cell* **49**, 65-73.

**Lawrence, P. A., Bodmer, R. and Vincent, J. P.** (1995). Segmental patterning of heart precursors in Drosophila. *Development* **121**, 4303-4308.

**Llimargas, M.** (2000). Wingless and its signalling pathway have common and separable functions during tracheal development. *Development* **127**, 4407-4417.

**McLachlan, R. W., Kraemer, A., Helwani, F. M., Kovacs, E. M. and Yap, A. S.** (2007). E-cadherin adhesion activates c-Src signaling at cell-cell contacts. *Mol. Biol. Cell* **18**, 3214-3223.

**Molenaar, M., van de Wetering, M., Oosterwegel, M., Peterson-Maduro, J., Godsave, S., Korinek, V., Roose, J., Destree, O. and Clevers, H.** (1996). XTcf-3 transcription factor mediates beta-catenin-induced axis formation in Xenopus embryos. *Cell* **86**, 391-399.

**Oda, H. and Tsukita, S.** (1999a). Dynamic features of adherens junctions during Drosophila embryonic epithelial morphogenesis revealed by a Dalpha-catenin-GFP fusion protein. *Dev. Genes Evol.* **209**, 218-225.

**Oda, H. and Tsukita, S.** (1999b). Nonchordate classic cadherins have a structurally and functionally unique domain that is absent from chordate classic cadherins. *Dev. Biol.* **216**, 406-422.

**Oda, H., Uemura, T., Harada, Y., Iwai, Y. and Takeichi, M.** (1994). A Drosophila homolog of cadherin associated with armadillo and essential for embryonic cell-cell adhesion. *Dev. Biol.* **165**, 716-726.

**Pai, L. M., Orsulic, S., Bejsovec, A. and Peifer, M.** (1997). Negative regulation of Armadillo, a Wingless effector in Drosophila. *Development* **124**, 2255-2266.

**Peifer, M., Rauskolb, C., Williams, M., Riggleman, B. and Wieschaus, E.** (1991). The segment polarity gene armadillo interacts with the wingless signaling pathway in both embryonic and adult pattern formation. *Development* **111**, 1029-1043.

**Perrimon, N., Noll, E., McCall, K. and Brand, A.** (1991). Generating lineage-specific markers to study Drosophila development. *Dev. Genet.* **12**, 238-252.

**Piwnica-Worms, H., Saunders, K. B., Roberts, T. M., Smith, A. E. and Cheng, S. H.** (1987). Tyrosine phosphorylation regulates the biochemical and biological properties of pp60c-src. *Cell* **49**, 75-82.

**Rabut, G. and Ellenberg, J.** (2005). Photobleaching techniques to study mobility and molecular dynamics of proteins in live cells: FRAP, iFRAP, and FLIP. In *Live Cell Imaging: A Laboratory Manual* (ed. R. D. Goldman and D. L. Spector), pp. 101-126. Cold Spring Harbor, New York: Cold Spring Harbor Press.

**Ribeiro, C., Neumann, M. and Affolter, M.** (2004). Genetic control of cell intercalation during tracheal morphogenesis in Drosophila. *Curr. Biol.* **14**, 2197-2207.

**Sakata, T., Sakaguchi, H., Tsuda, L., Higashitani, A., Aigaki, T., Matsuno, K. and Hayashi, S.** (2004). Drosophila Nedd4 regulates endocytosis of notch and suppresses its ligand-independent activation. *Curr. Biol.* **14**, 2228-2236.

**Samakovlis, C., Hacohen, N., Manning, G., Sutherland, D. C., Guillemin, K. and Krasnow, M. A.** (1996). Development of the Drosophila tracheal system occurs by a series of morphologically distinct but genetically coupled branching events. *Development* **122**, 1395-1407.

**Shiga, Y., Tanaka-Matakatsu, M. and Hayashi, S.** (1996). A nuclear GFP/ beta-galactosidase fusion protein as a marker for morphogenesis in living Drosophila. *Dev. Growth Differ.* **38**, 99-106.

**Simon, M. A., Drees, B., Kornberg, T. and Bishop, J. M.** (1985). The nucleotide sequence and the tissue-specific expression of Drosophila c-src. *Cell* **42**, 831-840.

**Takahashi, M., Takahashi, F., Ui-Tei, K., Kojima, T. and Saigo, K.** (2005). Requirements of genetic interactions between Src42A, armadillo and shotgun, a gene encoding E-cadherin, for normal development in Drosophila. *Development* **132**, 2547-2559.

**Takeichi, M.** (1991). Cadherin cell adhesion receptors as a morphogenetic regulator. *Science* **251**, 1451-1455.

**Tanaka-Matakatsu, M., Uemura, T., Oda, H., Takeichi, M. and Hayashi, S.** (1996). Cadherin-mediated cell adhesion and cell motility in *Drosophila* trachea regulated by the transcription factor Escargot. *Development* **122**, 3697-3705.

**Tateno, M., Nishida, Y. and Adachi-Yamada, T.** (2000). Regulation of JNK by Src during Drosophila development. *Science* **287**, 324-327.

**Tepass, U., Gruszynski-DeFeo, E., Haag, T. A., Omatyar, L., Torok, T. and Hartenstein, V.** (1996). shotgun encodes Drosophila E-cadherin and is preferentially required during cell rearrangement in the neurectoderm and other morphogenetically active epithelia. *Genes Dev.* **10**, 672-685.

**Thomas, S. M. and Brugge, J. S.** (1997). Cellular functions regulated by Src family kinases. *Annu. Rev. Cell Dev. Biol.* **13**, 513-609.

**Toba, G., Ohsako, T., Miyata, N., Ohtsuka, T., Seong, K. H. and Aigaki, T.** (1999). The gene search system. A method for efficient detection and rapid molecular identification of genes in Drosophila melanogaster. *Genetics* **151**, 725-737.

**Uemura, T., Oda, H., Kraut, R., Hayashi, S., Kotaoka, Y. and Takeichi, M.** (1996). Zygotic Drosophila E-cadherin expression is required for processes of dynamic epithelial cell rearrangement in the Drosophila embryo. *Genes Dev.* **10**, 659-671.

**van de Wetering, M., Cavallo, R., Dooijes, D., van Beest, M., van Es, J., Loureiro, J., Ypma, A., Hursh, D., Jones, T., Bejsovec, A. et al.** (1997). Armadillo coactivates transcription driven by the product of the Drosophila segment polarity gene dTCF. *Cell* **88**, 789-799.

**Wada, A., Kato, K., Uwo, M. F., Yonemura, S. and Hayashi, S.** (2007). Specialized extraembryonic cells connect embryonic and extraembryonic epidermis in response to Dpp during dorsal closure in Drosophila. *Dev. Biol.* **301**, 340-349.

**Wang, Y., Botvinick, E. L., Zhao, Y., Berns, M. W., Usami, S., Tsien, R. Y. and Chien, S.** (2005). Visualizing the mechanical activation of Src. *Nature* **434**, 1040-1045.

**Wodarz, A., Stewart, D. B., Nelson, W. J. and Nusse, R.** (2006). Wingless signaling modulates cadherin-mediated cell adhesion in Drosophila imaginal disc cells. *J. Cell Sci.* **119**, 2425-2434.

**Yamada, S., Pokutta, S., Drees, F., Weis, W. I. and Nelson, W. J.** (2005). Deconstructing the cadherin-catenin-actin complex. *Cell* **123**, 889-901.

**Zallen, J. A. and Wieschaus, E.** (2004). Patterned gene expression directs bipolar planar polarity in Drosophila. *Dev. Cell* **6**, 343-355.